at large R. In very covalent molecules, whose component atoms are quite different in size, the second term should contribute significantly to the dipole moment. The model should apply equally well to molecules ranging from highly polar to homonuclear. In the latter case the dipole moment given by eq 71 reduces to zero as it should. This model in conjunction with experimental data can be used to explain trends in charge distributions in diatomic molecules across the periodic table. This possibility is explored in part 2 of this series.

Acknowledgment. The authors wish to thank Dr. Luis Kahn, Dr. C. W. Kern, and Mr. Rudolf Goldflam for helpful comments. They also wish to acknowledge the support of Battelle Memorial Institute and the Robert A. Welch Foundation through Grant No. E-397.

References and Notes

(1) (a) Address correspondence to the University of Houston; (b) Battelle Memorial Institute; (c) University of Houston.
(2) E. S. Rittner, *J. Chem. Phys.*, **19**, 1030 (1951).
(3) P. Brumer and M. Karplus, *J. Chem. Phys.*, **58**, 3903 (1973).
(4) J. Murrell and G. Shaw, *J. Chem. Phys.*, **46**, 1768 (1967); J. Murrell, M. Randic, and D. R. Williams, *Proc. R. Soc. London, Ser. A*, **284**, 566 (1965); L. Salem, *Discuss. Faraday Soc.*, **40**, 150 (1965); J. I. Musher and L. Salem, *J. Chem. Phys.*, **44**, 2943 (1966); R. Yaris, *ibid.*, **44**, 3894 (1966).
(5) H. E. DeWijn, *J. Chem. Phys.*, **44**, 810 (1966).
(6) R. L. Matcha, W. D. Lyon, and J. O. Hirschfelder, *J. Chem. Phys.*, **43**, 1101 (1965).
(7) R. Makinson and J. Turner, *Proc. Phys. Soc., London, Sect. A*, **66**, 857 (1953); R. Sternheimer, *Phys. Rev.*, **96**, 951 (1954).
(8) R. L. Matcha and R. K. Nesbet, *Phys. Rev.*, **160**, 72 (1967).
(9) For notation and phase conventions, see R. L. Matcha, C. W. Kern, and D. M. Schrader, *J. Chem. Phys.*, **51**, 2152 (1969).

Theory of the Chemical Bond. 2. Dipole Moments of Alkali Halide Molecules, Bond Polarity, and Differential Charge Affinity

Robert L. Matcha*[1a,b] and Stephen C. King, Jr.[1c]

Contribution from the Department of Chemistry, University of Houston, Houston, Texas 77004, and Battelle Memorial Institute, Columbus, Ohio 44201.
Received August 27, 1974

Abstract: An accurate dipole moment model is used to analyze dipole moments of alkali halide molecules. It is found that for these molecules the effective charge transferred during molecular formation, f, ranges systematically from 0.76 to 0.99 in an order predictable from the periodic table. The f's are related to atomic parameters by the equation $f = (q_M - q_X)/2$ where q_α is the ideal charge of atom α. The model is found to predict equilibrium dipole moments and slopes for alkali halides which differ on the average from experimental values by 0.33 and 1.5%, respectively. A complete table of alkali halide dipole moments is constructed; given are coefficients in the equation $\mu_{v,J} = \mu_0 + \mu_1(v + \frac{1}{2}) + \mu_{11}(v + \frac{1}{2})^2 + \mu_0{}^J J(J+1) + \mu_1{}^J J(J+1)(v + \frac{1}{2})$, where v and J are vibrational and rotational quantum numbers, respectively. The model is compared with several other dipole moment models. The model leads to a plausible interpretation of the signs of equilibrium dipole moments for such molecules as CF which have appeared to violate chemical intuition. A quantitative procedure for resolving chemical bonds into ionic and covalent components is proposed. The method derives from an analysis of alkali halide dipole moment measurements. Bonds are classified according to their polarity $f = (q_A - q_B)/2$ and their covalency $c = (q_A + q_B)/2$. A new concept, the differential charge affinity, is introduced to explain trends in the bond polarities of alkali halide molecules. The relationship of this property to ionization potentials and electron affinities is explored. A comparison of bond polarities and differential charge affinities with the older concepts of ionic character and electronegativity is given.

The relationship of atomic interactions and molecular properties to bond parameters and charge distributions can be studied with the aid of appropriate models in conjunction with experimental data. Models of molecular properties are usually based on qualitative classical electrodynamic arguments and are self limiting in that they frequently do not incorporate important quantum mechanical effects. It is therefore desirable to derive models within the framework of a quantum mechanical formalism.

One procedure for facilitating this endeavor was developed in the first paper[2] of this series (1). There, a model relating dipole moments to bond lengths in diatomic molecules was derived using a formalism termed implicit perturbation theory. The model has the form

$$\mu = fR\left(1 - \frac{\alpha_A + \alpha_B}{R^3}\right) + cR\left(2\frac{z_{cv}}{R} - 7\frac{(\alpha_A - \alpha_B)}{R^3}\right) + ke^{-\gamma R} \quad (1)$$

The first term represents the dipole moment associated with two hypothetical polarizable charges $\pm f$ located at the two nuclei. The second term describes the dipole moment associated with an overlap charge $-2c$ located a distance $-z_{cv}$ toward A from the geometric center of the molecule. This charge induces moments in the partially charged ions. The third term approximates collision-induced moments at distances less than R_e in addition to effects due to kinetic energy variations with R.

In this paper we introduce a dipole moment model appropriate to highly polar molecules and evaluate it by analyzing experimental dipole moment data. The functional form we adopt is suggested both by the quantum mechanical model and the classical arguments of Rittner.[3a] Constants are obtained empirically by demanding the best possible fit with experimenta alkali halide data. Trends among the fitted constants are examined graphically to determine the correlation between actual and expected behavior.

Based on an analysis of the constants, we attempt to deduce new information pertaining to bond formation and to evaluate

Table I. Calculated and Experimental Coefficients of Dipole Moment Expansion in Powers of $(v + \frac{1}{2})$ and $J(J + 1)$

	μ_0, D		μ_1, D		μ_{11}, D			
Molecule	Theor	Exptl	Theor	Exptl	Theor	Exptl	$\mu_0^J \times 10^5$, D	$\mu_1^J \times 10^7$, D
$^7Li^{19}F$	6.152 84	(6.284 0)[a]	0.077 38	(0.081 53)[a]	0.000 60	(0.000 44)[a]	4.901 79	5.293 98
$^6Li^{35}Cl$	7.127 79	(7.085 3)[a]	0.085 23	(0.086 83)[a]	0.000 38	(0.000 56)[a]	4.818 07	7.524 83
$^6Li^{79}Br$	7.209 59	(7.226 2)[b]	0.086 32	(0.083 18)[b]	−0.000 19	(0.000 57)[b]	4.691 01	−3.325 76
$^7Li^{127}I$	7.361 02	(7.387)[c]	0.077 27	(0.074)[h]	0.000 31		3.463 60	4.278 02
$^{23}Na^{19}F$	8.128 78	(8.123 49)[d]	0.063 22	(0.06436)[d]	0.000 36	(0.000 37)[d]	2.091 51	5.248 26
$^{23}Na^{35}Cl$	8.917 40	(8.972 1)[a]	0.060 05	(0.059 63)[a]	0.000 16	(0.000 17)[a]	1.564 84	1.869 57
$^{23}Na^{79}Br$	9.073 32	(9.091 8)[a]	0.053 14	(0.053 1)[a]	0.000 13		1.184 67	1.062 90
$^{23}Na^{127}I$	9.241 86	(9.210 3)[a]	0.050 44	(0.050 7)[a]	0.000 11		1.017 96	1.060 82
$^{39}K^{19}F$	8.554 83	(8.558 32)[e]	0.068 83	(0.068 41)[e]	0.000 25	(0.000 26)[e]	1.942 17	3.126 29
$^{39}K^{35}Cl$	10.216 71	(10.239 11)[f]	0.059 69	(0.059 66)[f]	0.000 16	(0.000 19)[f]	1.142 02	1.289 66
$^{39}K^{79}Br$	10.600 62	(10.602 87)[e]	0.049 72	(0.050 25)[e]	0.000 12		0.754 13	0.778 60
$^{39}K^{127}I$	11.070 14	(11.05)[g]	0.045 54		0.000 11		0.594 89	0.604 04
$^{85}Rb^{19}F$	8.529 55	(8.513 1)[a]	0.066 26	(0.066 50)[a]	0.000 23	(0.000 26)[a]	1.598 04	2.058 35
$^{85}Rb^{35}Cl$	10.449 78	(10.483)[a]	0.054 15	(0.054)[a]	0.000 14		0.820 76	0.911 43
$^{85}Rb^{79}Br$	10.955 53		0.041 49		0.000 10		0.456 31	0.409 14
$^{85}Rb^{127}I$	11.637 94		0.035 60		0.000 08		0.316 69	0.298 54
$^{133}Cs^{19}F$	7.831 06	(7.842)[a]	0.072 75	(0.072 29)[a]	0.000 27		1.685 41	2.342 52
$^{133}Cs^{35}Cl$	10.416 78	(10.392)[i]	0.057 61	(0.056)[i]	0.000 16		0.769 21	0.892 01
$^{133}Cs^{79}Br$	11.293 49		0.041 53		0.000 11		0.373 81	0.337 17
$^{133}Cs^{127}I$	12.435 61		0.033 83		0.000 10		0.228 82	0.241 60

[a] Reference 12. [b] Reference 15. [c] Reference 16. [d] Reference 6. [e] Reference 11. [f] Reference 5. [g] Reference 14. [h] Estimated from $^6Li^{127}I$ data. [i] Reference 4.

the quantum mechanical model. The independent procedures of deriving models semiempirically and quantum mechanically are complementary. In fact, the model developed in this paper preceded and suggested much of the formal development in part 1.

Our analysis yields new insight into the traditional concepts of ionic and covalent character and electronegativity. It also suggests the existence of a new characteristic atomic property, the differential charge affinity. The latter property is closely related to the partial charge acquired by an atom during molecular formation.

Analysis of Model Parameters

A proper analysis of the dipole moment model requires accurate experimental dipole moment curve data for a series of molecules. Such curves can be extracted from appropriate spectroscopic and molecular beam measurements. The latter yield the dipole moment expansions

$$\mu_{v,J} = \mu_0 + \mu_I(v + \tfrac{1}{2}) + \mu_{II}(v + \tfrac{1}{2})^2 + \mu_0{}^J J(J+1) + \mu_I{}^J J(J+1)(v + \tfrac{1}{2}) + \ldots \quad (2)$$

where v and J are vibrational and rotational quantum numbers and $\mu_\alpha{}^\nu$ are expansion coefficients. These data can be coupled with spectroscopic measurements to obtain dipole moment expansions about R_e having the form

$$\mu = \mu_e + \alpha\xi + \beta\xi^2 + \ldots \quad (3)$$

where $\xi = (R - R_e)/R_e$. Using Rayleigh Schröedinger perturbation theory it can be shown[3b] that the coefficients in eq 2 and 3 are related to spectroscopic constants B_e and ω_e by the equations, $\mu_0 = \mu_e$,

$$\mu_1 = \frac{B_e}{\omega_e}[-3\alpha a_1 + 2\beta] \quad (4)$$

$$\mu_{11} = \frac{B_e{}^2}{\omega_e{}^2}\left[\alpha\left(-\frac{45}{2}a_1{}^3 + 39a_1a_2 - 15a_3\right) + \beta(15a_1{}^2 - 6a_2)\right] \quad (5)$$

$$\mu_0{}^J = 4\alpha B_e{}^2/\omega_e{}^2 \quad (6)$$

and

$$\mu_1{}^J = \frac{B_e{}^3}{\omega_e{}^3}[\alpha(48 + 54a_1 - 54a_1{}^2 - 48a_2) - \beta(12 + 36a_1)] \quad (7)$$

where $B_e = h^2/8\pi^2\mu R_e{}^2$, $\omega_e = (4a_0B_e)^{1/2}$, and μ is the reduced mass. The constants a_0, a_1, a_2, and a_3 are defined by the expansion,

$$U = a_0\xi^2(1 + a_1\xi + a_2\xi^2 + a_3\xi^3 + \ldots) \quad (8)$$

where U is the potential energy of the system.

Equations 3-8 comprise a set of simultaneous linear equations which can be solved for α and β to obtain μ as a function of R. This requires considerable experimental data. For the alkali halides extensive spectroscopic and dipole moment measurements have been made.[4-16] The results of these are tabulated in Table I and in columns 2-6 of Table II. However, even for this rather select group of molecules no experimental measurements of $\mu_0{}^J$ and $\mu_1{}^J$ are available and only scattered measurements of μ_{II} exist. Thus, except in a few cases where available data allow a more accurate treatment, we utilize the approximation

$$\mu = A + BR \quad (9)$$

where

$$A = \mu_0 + \mu_1\omega_e/3a_1B_e \quad (10)$$

and

$$B = -\mu_1\omega_e/3a_1B_eR_e \quad (11)$$

Equation 9 is derived by substituting α from eq 4 into eq 3, setting $\beta = 0$ and rearranging.

Clearly, the information content in eq 9 is limited and insufficient to permit examination of all features of the full dipole moment model. Thus we have adopted the simpler expression, applicable to very polar molecules,

$$\mu = fR\left(1 - \frac{a}{R^3} + \frac{b}{R^6}\right) \quad (12)$$

Table II. Spectroscopic Constants for Alkali Halides and Sum of Partial Ionic Radii

Molecule	a_1	a_2	a_3	B_e, cm^{-1}	ω_e, cm^{-1}	R_e, a_0	$r_M + r_X$	% difference
$^7Li^{19}F$	−2.7239[a]	6.6[a]	−17.2[a]	1.345 39[a]	922[a]	2.955 28[a]	3.26	10.3
$^6Li^{35}Cl$	−2.72[b]	5.3[b]	−9[b]	0.804 40[b]	684.1[c]	3.818 54[b]	3.97	3.9
$^6Li^{79}Br$	−2.71[d]	6.8[d]	−19[d]	0.640 300[d]	576.0[d]	4.101 55[d]	4.27	4.1
$^7Li^{127}I$	−2.70[e]	5.0[d]	−8[d]	0.443 176[d]	490[d]	4.520 13[d]	4.69	3.7
$^{23}Na^{19}F$	−3.133[a]	6.43[a]	−9.2[a]	0.436 903[a]	536.10[a]	3.639 53[a]	3.53	3.0
$^{23}Na^{35}Cl$	−3.076[e]	6.47[e]	−11.0[e]	0.218 064[e]	364.60[e]	4.461 49[e]	4.24	4.9
$^{23}Na^{79}Br$	−3.05[d]	6.5[d]	−12[d]	0.151 253[d]	298.49[d]	4.728 19[d]	4.54	3.9
$^{23}Na^{127}I$	−3.02[d]	5.9[d]	−8[d]	0.117 805[d]	259.20[d]	5.123 94[d]	4.96	3.1
$^{39}K^{19}F$	−3.1157[a]	6.34[a]	−9.6[a]	0.279 938[a]	426.04[a]	4.103 48[a]	4.16	1.4
$^{39}K^{35}Cl$	−3.226[e]	6.96[e]	−12.0[e]	0.128 635[e]	279.80[e]	5.039 56[e]	4.87	3.3
$^{39}K^{79}Br$	−3.24[d]	6.9[d]	−11[e]	0.081 221[d]	219.17[d]	5.330 53[d]	5.17	1.3
$^{39}K^{127}I$	−3.25[d]	6.9[d]	−11[d]	0.060 875[d]	186.53[d]	5.759 59[e]	5.59	2.9
$^{85}Rb^{19}F$	−3.1347[a]	6.58[a]	−11.4[a]	0.210 665[a]	373.27[a]	4.290 32[a]	4.53	5.6
$^{85}Rb^{35}Cl$	−3.297[e]	7.08[e]	−11.5[e]	0.087 640[e]	233.34[e]	5.266 57[e]	5.24	0.5
$^{85}Rb^{79}Br$	−3.33[d]	7.3[d]	−13[d]	0.047 528[d]	169.46[d]	5.564 80[d]	5.54	0.3
$^{85}Rb^{127}I$	−3.34[d]	7.2[d]	−11[d]	0.032 833[d]	138.51[d]	6.003 46[d]	5.96	0.7
$^{133}Cs^{19}F$	−3.0324[a]	5.65[a]	−7.2[a]	0.184 369[a]	352.56[a]	4.432 09[a]	4.98	12.4
$^{133}Cs^{35}Cl$	−3.317[e]	6.92[e]	−10.0[e]	0.072 091[e]	214.22[e]	5.492 34[e]	5.69	3.6
$^{133}Cs^{79}Br$	−3.38[e]	7.6[d]	−14[d]	0.036 069[d]	149.50[d]	5.805 74[e]	5.99	3.1
$^{133}Cs^{127}I$	−3.43[d]	7.6[d]	−13[d]	0.023 627[d]	119.195[d]	6.264 85[d]	6.41	2.2
								⟨% diff⟩ 3.7

[a] Reference 13. [b] Reference 7. [c] Determined from relationship $\omega_e = 4a_0B_e$ using data from ref 7. [d] eference 10. [e] Reference 9.

Table III. Experimental Values of f, a, and b and Calculated Values of f

Molecule	f	a, Å^3	b, Å^6	$f = \frac{1}{2}(q_M - q_X)$	f_{approx}
LiF	0.8730	0.2722	0.4360	0.84	0.92
LiCl	0.8188	1.2622	3.0505	0.815	0.88
NaF	0.8925	0.2401	0.9129	0.888	0.91
NaCl	0.8633	1.3623	3.4746	0.865	0.86
NaBr	0.8428	1.9677	5.7500	0.843	0.84
NaI	0.8116	3.1420	11.5882	0.812	0.81
KF	0.9331	1.5554	3.2760	0.933	0.94
KCl	0.9077	2.7788	9.8281	0.908	0.90
RbF	0.9435	2.4897	5.5106	0.943	0.95
RbCl	0.9181	3.9542	16.7424	0.918	0.90
CsF	0.9891	4.7630	12.1388	0.989	0.98
CsCl	0.9627	6.9745	33.0768	0.964	0.92

This model approximates a system of two polarizable positive and negative ions whose charges differ by $2f$. The R^{-6} term can be viewed as a higher term in a multipole expansion. This expression is reminiscent of Rittner's model[3a] [see eq 24]. However, a is not assumed in advance to be a sum of ionic polarizabilities nor b a product. Nor is f assumed to be unity.

To obtain values of f, a, and b from the experimental curves we equate zeroth, first, and second derivatives of eq 12 to corresponding derivatives of eq 9, all evaluated at R_e, and solve the resultant equations. Following this procedure we have determined the coefficients tabulated in columns 2–4 of Table III.

Definition Coordinate Analysis

The theoretical development in paper 1 suggests that certain trends should be evident in the f, a, and b coefficients. For example, a is expected to be a sum of atomic polarizabilities and f is expected to be related to atomic charge distributions. To discern systematic trends we use an empirical procedure which we call a definition coordinate analysis. Our primary aim is to ascertain functional relationships between f, a, and b and parameters identifiable with atomic properties and charges.

In this procedure we graph appropriate constants against coordinates representing hypothetical parameters whose physical significance remains to be established. In Figures 1 and 2 we apply the procedure to an analysis of f. At an arbitrary point along the abscissa in Figure 1, a vertical line was drawn with height corresponding to f for CsF. At another arbitrary point, a vertical line was drawn with height corresponding to f for NaF. On this line the NaCl, NaBr, and NaI f's were plotted. A slanted line was next drawn through the points representing CsF and NaF. On this line f values of RbF and KF were marked and through these vertical lines were drawn. Finally, slanted lines parallel to the line through CsF and NaF were drawn through NaCl, NaBr, and NaI. On the slanted line through NaCl f values for LiCl, KCl, RbCl, and CsCl were plotted. Similarly f values of the remaining molecules were included in the figure. According to these constructions, the abscissa represents a hypothetical quantity having the same value for all the sodium halides but varying linearly with f among the alkali chlorides. An axis used in this way we call a definition coordinate. Figure 2 was constructed in a similar fashion beginning with NaF and NaI.

Figures 1 and 2 are consistent with eq 48 in part 1 in that the f's appear as differences in quantities associated with the atoms. In addition, the figures imply that this difference is obtainable for each of the alkali halides from constants associated with the component atoms. We call these constants ideal charges q and write

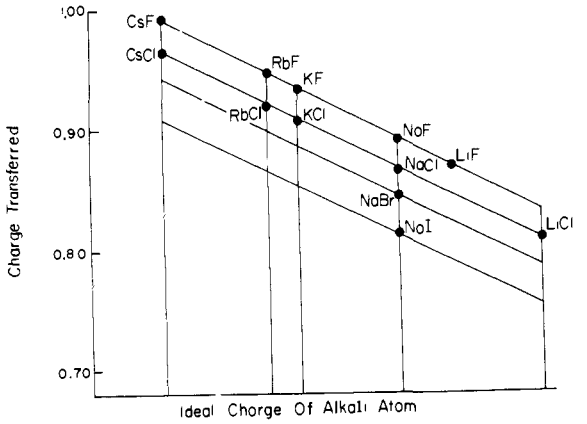

Figure 1. Variation of fractional electron charge transferred with ideal charge of alkali atom. The heights of curves are related to the ideal charge of halogen atoms.

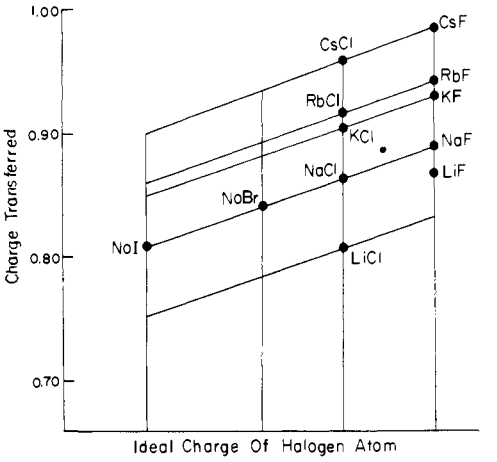

Figure 2. Variation of fractional electron charge transferred with ideal charge of halide atom. The heights of curves are related to the ideal charge of alkali atoms.

Table IV. Computed Values of Ideal Charges for Alkali and Halide Atoms

Atom	q_M	Atom	q_X
Li	0.680	F	−1.000
Na	0.776	Cl	−0.950
K	0.866	Br	−0.910
Rb	0.886	I	−0.848
Cs	0.978		

$$f = (q_M - q_X)/2 \tag{13}$$

Since the charges appear only as differences it is necessary to arbitrarily assign a value to one of the elements. Thus we assign fluorine an ideal charge of −1. The remaining ideal charges can be determined from eight f's. For example, $q_{Rb} + 1 = 2f_{RbF} = 1.886$, thus $q_{Rb} = 0.886$. In this manner we have determined the remaining ideal charges for alkali and halide ions in alkali halide molecules and listed them in Table IV. As can be seen from Figure 1, the f's of LiCl and LiF imply different q's. Thus the tabulated value of q_{Li} is somewhat of an average chosen to optimize the agreement between the experimental dipole moments and those predicted by the model.

The q's given in Table IV were used to compute the f's given in the fourth column of Table III. Included in the table are the experimental f's. The agreement is quite close except for LiF where a 4% difference exists. It should be pointed out that the f values are quite sensitive to the experimental data. A 1% variation in μ_I can produce a 1% variation in f. The error estimate in μ_I for RbCl is as one example 5½% of the magnitude of μ_I. However, experimental error probably is not the cause[17] of the anomalous f for LiF.

The coefficient a should be approximately a sum of effective atomic polarizabilities. In fact, by an analysis similar to the preceding, we find that a good representation of a is given by the expression

$$a = \alpha_M(1 + k_F) + \alpha_X \tag{14}$$

where k_F is a coupling factor with value zero except for the molecules RbF, CsF, KF, and NaF. In these cases it is approximately equal to $-\frac{1}{4}$ for Rb, Cs, and K and $-\frac{3}{4}$ for Na. The effective polarizabilities are listed in column 7 of Table V. Pauling's values are listed under the column α_p. The appearance of the factor $1 + k_F$ is somewhat annoying but not too surprising considering the various molecular terms appearing in the dipole moment model developed formally. (owever, it is possible the parameter k_F is an artifact of the model related to the fb/R^5 term [see General Reliability of Constants].)

A comparison of columns 7 and 8 in Table V indicates that the alkali ion polarizabilities determined from coefficients a are larger than Pauling's values while the halide ion polarizabilities are smaller. To understand why this should be it is instructive to examine eq 1. There we note that the term proportional to $-1/R^3$ is $(f + 7c)\alpha_A + (f - 7c)\alpha_B$. Our observed polarizabilities are true polarizabilities weighted by the factors $f + 7c$ and $f - 7c$. This formula was derived assuming a covalent charge at $R/2$. In actuality, the smaller the relative size of the alkali atom the larger the weighting factor since the covalent charge is located a variable distance from the nucleus. Thus we observe lithium polarizability six times greater than Pauling's and a cesium polarizability 2.5 times greater. Conversely, Pauling's fluoride polarizability is approximately ten times greater than our value while the iodine value is 2.5 times greater. The fluorine discrepancy is greater than the iodine

Table V. Ionic Constants for Alkali Metals and Halogens

Ion	γ	r, a_0	r_p, a_0	R, Å	$\frac{4}{3}\pi R^3$	α, Å^3	α_p, Å^3
Li^+	−0.400 48	1.51	0.903[a]	0.3629	0.2002	0.18	0.029
Na^+	0.058 27	1.78	1.559	0.4861	0.4811	0.53	0.181
K^+	1.098 61	2.41	2.137	0.7655	1.8788	1.92	0.84
Rb^+	1.710 18	2.78	2.364	0.9297	3.3662	3.17	1.42
Cs^+	2.460 40	3.23	2.591	1.1312	6.0631	6.20	2.44
F^-	0.000 00	1.75	1.841	0.2978	0.1106	0.09	1.05
Cl^-	1.181 27	2.46	2.901	0.5743	0.7943	0.90	3.69
Br^-	1.687 46	2.76	3.192	0.6928	1.3928	1.47	4.81
I^-	2.385 82	3.18	3.623	0.8563	2.6297	2.56	7.16

[a] Determined by Honig et al. using Pauling's methods, ref 14. [b] L. Pauling, *Proc. R. Soc. London, Ser. A*, **114**, 191 (1927).

Table VI. Computed Values of f, a, b, μ_e, α, and β for the Alkali Halides

Molecule	f	a, Å^3	b, Å^6	μ_e, D	α, D	β, D
LiF	0.840	0.2700	0.669 99	6.152 84	5.755 20	2.998 35
LiCl	0.815	1.0800	2.183 19	7.127 79	8.711 81	0.694 15
LiBr	0.792	1.6500	3.621 83	7.209 59	9.490 40	0.293 70
LiI	0.764	2.7400	7.281 52	7.361 02	10.585 41	−0.153 39
NaF	0.888	0.2225	1.060 00	8.128 78	7.872 63	1.791 64
NaCl	0.863	1.4300	3.454 02	8.917 40	10.936 45	−0.262 38
NaBr	0.843	2.0000	5.730 08	9.073 32	11.534 23	−0.331 47
NaI	0.812	3.0900	11.520 06	9.241 86	12.320 03	−0.319 13
KF	0.93	1.5300	3.000 00	8.554 83	11.246 19	−0.185 28
KCl	0.908	2.8200	9.775 51	10.216 71	13.508 03	−0.446 76
KBr	0.888	3.3900	16.217 16	10.600 62	13.728 08	0.358 23
KI	0.857	4.4800	32.603 84	11.070 14	13.963 77	1.698 82
RbF	0.943	2.4675	5.529 96	8.529 55	12.542 64	−0.275 96
RbCl	0.918	4.0700	18.019 42	10.449 78	14.545 59	0.156 80
RbBr	0.898	4.6400	28.893 47	10.955 53	14.502 26	1.518 29
RbI	0.867	5.7300	60.099 41	11.637 94	14.090 11	4.508 24
CsF	0.989	4.7400	11.709 96	7.831 06	15.407 66	−0.522 16
CsCl	0.964	7.1000	38.157 03	10.416 78	16.980 23	1.103 41
CsBr	0.944	7.6700	63.300 93	11.293 49	16.054 88	4.675 89
CsI	0.913	8.7600	127.263 53	12.435 61	14.559 37	10.418 46

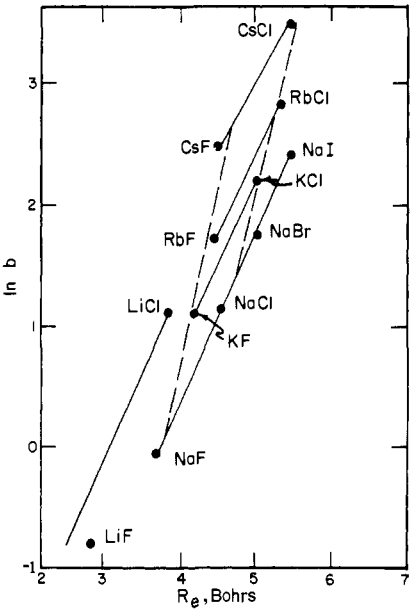

Figure 3. Plot of ln b vs. R_e for alkali halide molecules.

because the interfering covalent charge is closer to the former atom than the latter.

A definition coordinate analysis of b indicates that this constant is related to atomic parameters γ_M and γ_X by the equation

$$b = \exp(\gamma_M + \gamma_X) \tag{15}$$

Using the coefficients listed in Table III, we have determined the γ constants tabulated in Table V (information on eight molecules was needed for this determination). The γ's are closely related to the internuclear separation at which the charge cloud overlap begins affecting μ (roughly R_e). This is evident in Figure 3 where we have plotted ln b vs. R_e. This may be nature's way of saying that it prefers e^{-R} to R^{-5} as the third term in the model. The exponential seems to appear whether or not it is included explicity.

An analysis of the pattern displayed by Figure 3 indicates that the γ are approximately linearly related to effective ionic radii r. An averaging of slopes and intercepts of the various lines yields the approximate relationship

$$r = 3\gamma/5 + 7/4 \tag{16}$$

with r in bohrs. Using this equation we have calculated the effective ionic radii listed in Table V. In Table II sums of effective ionic radii are tabulated along with R_e and the percentage differences for alkali halides. The average difference is 3.7%. It should be noted that the effective radii, r, were determined using a criterion only indirectly related to R_e. There is a certain arbitrariness associated with splitting R_e into component radii. For example, the constant term 7/4 could be distributed differently. One third could be added to the halide radii and subtracted from the alkali radii. In that case the agreement between the Pauling radii, r_p in Table V, and the radii based on γ's would be quite good.

Using classical electrodynamic arguments[18] it can be shown that ionic polarizabilities are proportional to the ionic volumes. Since we have indicated that γ is linearly related to ionic radius, it follows that α is proportional to the cube of a linear function of γ. Indeed, the effective polarizability radii

$$R_M = 0.268\,55\gamma_M + 0.470\,45 \tag{17}$$

and

$$R_X = 0.234\,09\gamma_X + 0.297\,77 \tag{18}$$

obtained by graphing $\alpha^{1/3}$ vs. γ, substituted into

$$\alpha = 4/3\pi R^3 \tag{19}$$

yield the polarizabilities tabulated in the sixth column of Table V. These agree fairly well with the numbers extracted from the a's and listed in column 7. The average difference is about 6%.

Complete Table of Dipole Moments for Alkali Halides

Using the q's, α's, and γ's listed in Tables IV and V together with eq 13, 14, and 15, the constants f, a, and b have been computed for each of the alkali halide molecules and tabulated in Table VI. Included are computed values of μ_e, α, and β which correspond to the zeroth, first, and second derivative of eq 12 with respect to ξ, evaluated at $\xi = 0$.

Using the data from Tables VI and II and eqs. 4–7, coefficients corresponding to the dipole moment expansion in powers of $(v + 1/2)^n[J(J+1)]^m$ have been calculated and listed in Table I. No experimental values for the $\mu_\alpha{}^J$ constants are available. It can be seen that the agreement between computed and experimental values demonstrated in Table I is quite good. For small vibrational quantum numbers, the average difference

Table VII. Resolution of Dipole Moment Model as a Function of Internuclear Separation for KF[a]

R, a_0	μ_{pc}	fR	μ_{pol}	μ_{ov}	D	μ^b	μ_{exptl}[c]
2.0	5.083 08	4.742 52	−6.120 93	10.124 29	1.000 00	8.745 85	2.845 11
2.5	6.353 86	5.928 15	−3.917 40	3.317 53	1.000 00	5.328 27	4.203 59
3.0	7.624 63	7.113 78	−2.720 41	1.333 24	1.000 00	5.726 59	5.561 79
3.5	8.895 40	8.299 41	−1.998 67	0.616 84	1.000 00	6.917 57	6.919 72
4.0	10.166 18	9.485 04	−1.530 23	0.316 38	1.000 00	8.271 18	8.277 37
4.5	11.436 95	10.670 67	−1.209 07	0.175 57	1.000 00	9.637 15	9.634 75
5.0	12.707 71	11.856 30	−0.979 35	0.103 67	1.000 00	10.980 61	10.991 85
5.5	13.978 49	13.041 93	−0.809 38	0.064 37	1.000 00	12.296 90	12.348 68
6.0	15.249 26	14.227 56	−0.680 10	0.041 66	1.000 00	13.589 10	13.705 23
6.5	16.520 03	15.413 19	−0.579 50	0.027 92	1.000 00	14.861 59	15.061 50
7.0	17.790 81	16.598 82	−0.499 67	0.019 27	1.000 00	16.118 40	16.417 50
8.0	20.332 4	18.970 08	−0.382 56	0.009 89	1.000 00	18.597 38	19.128 67
9.0	22.873 89	21.341 34	−0.302 27	0.005 49	1.000 00	21.044 52	21.838 74
10.0	25.415 44	23.712 60	−0.244 84	0.003 24	1.000 00	23.470 96	24.547 70
12.0	30.498 53	28.455 13	−0.170 03	0.001 30	1.000 00	28.286 35	29.962 32
15.0	38.123 16	35.568 91	−0.108 82	0.000 43	.997 366	35.367 04	38.075 98
20.0	50.830 88	47.425 21	−0.061 21	0.000 10	.003 79	0.179 51	51.576 69
25.0	63.538 59	59.281 51	−0.039 17	0.000 03	.000 00	0.000 00	65.049 83
30.0	76.246 31	71.137 81	−0.027 20	0.000 01	.000 00	0.000 00	78.495 41

[a] All dipole moment data are expressed in debyes. [b] Sum of columns 3, 4, and 5 multiplied by D. [c] Values corresponding to $R < 3$ and $R > 10$ are probably not reliable.

between the calculated and experimental μ_v is on the order of ⅓%. Overall, the trends and systematic variations displayed among the calculated $\mu_0{}^J$ and $\mu_I{}^J$ indicate that values of these coefficients are reasonably reliable and accurate. It does appear, however, that the $\mu_I{}^J$ value for LiBr is anomalous. This may be due to poor experimental spectroscopic data. The value $a_2 = 5.2$ for LiBr yields the reasonable result $\mu_I{}^J = 6 \times 10^{-7}$ D. This value of a_2 was chosen to conform with the general pattern displayed in column 3 of Table II.

Resolution of Dipole Moment Model

It is instructive to examine in some detail the relative contributions to the dipole moment from each of three terms in eq 12. In Table VII we have listed the quantities

$$\mu_{pol} = -f[\alpha_M(1 + k_F) + \alpha_X]/R^2 \tag{20}$$

and

$$\mu_{0v} = f[\exp(\gamma_M + \gamma_X)]/R^5 \tag{21}$$

along with the sum μ and μ_{exptl} as a function of R for potassium fluoride. We have also tabulated eR, μ_{pc}. Although the variation of the various terms in Table VII is typical of all the alkali halides, the less than 5% difference between μ and μ_{exptl} over a range of several bohr radii is better than average. For a given molecule this difference is roughly proportional to the percent difference in μ_I indicated in Table I.

The experimental dipole moment is based on eq 3. The equation is only reliable near R_e since α and β were determined in this region. Consequently, at large R, the value of μ_{exptl} becomes greater than the limiting value eR. At large R, the dipole moment computed with the model in eq 12 is expected to be more reliable than μ_{exptl}. At small R (<3.0) the approximate nature of the overlap term ($1/R^5$) becomes apparent. Since the slope of this function is too pronounced, replacing R^{-5} by a term which depends exponentially on R markedly improves the agreement between μ and μ_{exptl} in the region $R < R_e$.

In Figure 4 the quantities in Table VII are plotted as a function of R. In order to get a physically realistic result for the computed curve in the charge transfer region, we have multiplied f by the damping factor

$$D = [1 + R^m/(R_D + C)^m]^{-1} \tag{22}$$

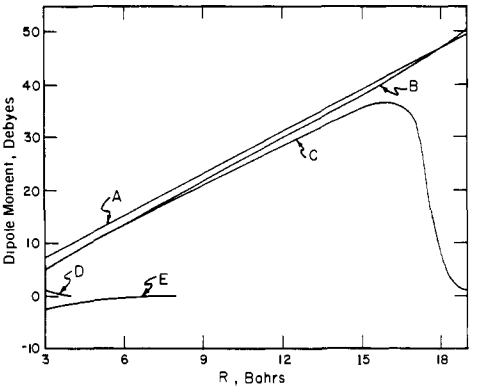

Figure 4. Variation of KF dipole moment with R. Curve A represents a point charge dipole, curve B represents the experimental curve, curve C represents the computed dipole using a damped f, curve D represents the overlap contribution, and curve E represents the effects of polarization.

choosing arbitrarily the values $R_D = 4R_e$, $m = 40$, and $C = 1$ for the various damping constants with R and C in bohrs. The purpose of this damping factor is to simulate the rapid decrease in dipole moment at distances beyond the curve crossing region when dissociating along the ground state potential curve. Values of D are listed in Table VII. If the damping factor is not included, the dipole moment, asymptotically, is that associated with two partially charged ions with charges $\pm f$.

Note that the overlap term is short ranged, being negligible at $R > R_e$. The polarization term is intermediate in nature, extending to about $2R_e$. Figure 4 indicates that the dipole model, eq 12, gives a reasonable facsimile of the dipole moment variation with R for alkali halides over a considerable distance.

Comparison of Dipole Moment Models

Based on the formal analysis in paper 1 it is possible to give a reasonably thorough analysis of both eq 12 and other dipole models indicating strong points and shortcomings. Models which we investigate are eq 12, the Rittner model,[3a] the truncated Rittner (T-Rittner) and dipole distortion models proposed by Brumer and Karplus,[19] and the DeWijn model.[20]

In constructing his model, Rittner viewed alkali halide molecules as consisting of two mutually polarizable spheres

Table VIII. Comparison of Calculated Dipole Moments

Molecule	μ(this paper)	|% error|	μ_{DW}	|% error|	$\mu_{T\text{-}Ritt}$[a]	|% error|	μ_{Ritt}[a]	|% error|
LiF	6.152 84[b]	2.08	6.04	2.40	5.3921	15.30	5.3106	15.56
LiCl	7.127 79	0.60	6.75	4.66	5.3306	24.80	5.2413	26.00
LiBr	7.209 59	0.05	7.10	1.80	5.4908	24.00	5.4083	25.10
LiI	7.361 02	0.35	7.44	0.72	5.4533	26.60	5.3752	27.60
NaF	8.128 8	0.06	8.02	1.23	7.6563	5.75	7.4922	7.76
NaCl	8.917 4	0.61	8.94	0.33	8.0037	10.80	7.7727	13.40
NaBr	9.073 3	0.19			8.1879	9.94	7.9597	12.50
NaI	9.241 9	0.32			8.2272	10.70	7.9917	13.20
KF	8.554 8	0.04	8.61	0.70	8.5042	0.63	8.0739	5.65
KCl	10.216 7	0.22	10.25	0.19	9.7492	4.77	9.1814	10.30
KBr	10.600 6	0.02	10.79	1.80	10.1370	4.38	9.5754	9.68
KI	11.070 1	0.18	11.41	3.25	10.5020	4.95	9.9214	10.20
RbF	8.529 5	0.18			8.6027	1.05	8.0013	6.01
RbCl	10.449 8	0.32			10.2250	2.46	9.4491	9.86
RbBr	10.955 5							
RbI	11.637 9							
CsF	7.831 1	0.12	7.96	1.38	8.2172	4.69	7.2781	7.26
CsCl	10.416 8	0.23	10.51	1.55	10.4740	1.11	9.3640	9.59
CsBr	11.293 5							
CsI	12.435 6		12.12		11.7270		10.6096	
	⟨% error⟩	0.34		1.67		9.49		13.07

[a] As calculated by Brumer and Karplus, ref 20. [b] Dipole moments are in debyes.

of charge ±1 in units of e separated by a distance R. Using classical electrodynamics he showed that for such a system the dipole moment is related to R by the equation

$$\mu_{Ritt} = R\left[1 - \frac{(\alpha_M + \alpha_X) - 4\alpha_M\alpha_X/R^3}{R^3 - 4\alpha_M\alpha_X/R^3}\right] \quad (23)$$

where α_M and α_X are ionic polarizabilities. This expression has a singularity at $R = (4\alpha_M\alpha_X)^{1/6}$ and is therefore clearly not valid for values of R in the neighborhood of this point. For large R we can expand in the form

$$\mu_{Ritt} = R\left[1 - \frac{\alpha_M + \alpha_X}{R^3} + \frac{4\alpha_M\alpha_X}{R^6} - \ldots\right] \quad (24)$$

The DeWijn model is the Rittner model with modified polarizabilities. DeWijn argues that the effect of mutual polarization is too strong in the Rittner model. Thus in his model he incorporates quenching of the orbitals in the halogen ion directed along the internuclear axis. Operationally speaking, he replaces α_X by $\frac{2}{3}\alpha_X$.

The T-Rittner model is eq 24 without the third term. In their formal analysis, Brumer and Karplus observed that overlap would introduce an exponential R dependence on the polarizability. Thus, they incorporated such a factor and called the resultant T-Rittner model with variable polarizabilities, the dipole distortion model.

Before examining each model separately it is useful to determine how well they reproduce experimental data. In Table VIII we have tabulated equilibrium dipole moments for alkali halides calculated with various models along with average errors. The latter measures 13.07% for the Rittner model, 9.49% for the T-Rittner model, 1.6% for the DeWijn model, and 0.33% for eq 12.

As a further comparison we have tabulated in Table IX values of μ_I computed with several models. In this case the average error measures 30.4% for the T-Rittner model, 26.7% for the DeWijn model, 24% for the dipole distortion model, and 1.5% for eq 12.

To determine the source of these errors let us examine each model separately in light of the formal theory developed in paper 1. Consider first of all eq 12. This model has three basic components. The long-range component is given by fR where f's are independent of R. However, according to eq 1 in this region μ should be given approximately by

$$\mu = (f + 2cz_{cv}/R)R \quad (25)$$

The second term is a covalent contribution to the dipole moment. This term is proportional to the difference in ionic radii and to the valence overlap. Thus, the more covalent the molecule and the greater the difference in ionic radii the larger the term. It is this effect that accounts for the anomalous f's observed in the lithium halides.

The second intermediate range component is given by $-fa/R^2$. The constant a, according to theory, is rather more complicated than a simple sum of ionic polarizabilities. It is this complex nature which may lead to the appearance of the coupling constant in eq 14. (See, however, the General Reliability of Constants section.)

The third component of eq 12 has the form fb/R^5. This term describes the short-range effect on the dipole moment which, as shown in paper 1, includes several factors. Since the overlap increases exponentially with decreasing R, the R^{-5} dependence is at best approximate. Thus at $R = 2$ in Table VII, the dipole moment of *KF* is 2.8451 while the model predicts 8.7458.

Let us consider the other models which for convenience we refer to as the "basically Rittner" or B-R models. Each of these has two components, a long range and an intermediate range. The long-range component is given by eR. Comparison with eq 1 shows that this term fails to account for both the charge transfer and the covalent effect. Consequently, the long-range portion of B-R models is appropriate to totally ionic ($f = 1$) molecules. It might be expected that discrepancies between predicted and experimental values of properties determined with these models would be correlated with the charge transfer occurring in a particular molecule. This is in fact the case. To demonstrate, by example, we define an approximate charge transferred f_{approx} by the equation

$$f_{approx} = 1 - \tfrac{1}{2}A \quad (26)$$

where A is the fractional error in μ_I computed with the dipole distortion model (see column 10 of Table IX). In Table III we have tabulated f_{approx}. The correlation between the f_{approx} and f is quite good. The average difference is 3.2%.

Table IX. Comparison of Computed and Experimental Values of μ_I for Alkali Halides (Dipole Moments are in Debyes)

Molecule	μ_I(exptl)[a]	μ_I(this paper)	|% error|	$\mu_{I(DW)}$	|% error|	$\mu_{I(T\text{-}Ritt)}$	|% error|	$\mu_{I(DD)}$	|% error|
$^{7}Li^{19}F$	0.081 53	0.077 38	5.1	0.098	20.2	0.100	22.6	0.095	16.5
$^{6}Li^{35}Cl$	0.086 83	0.085 23	1.8	0.110	26.7	0.121	39.3	0.107	23.2
$^{6}Li^{79}Br$	0.083 18	0.086 42	3.8	0.113	35.8	0.122	46.7	0.110	32.2
$^{7}Li^{127}I$	0.074	0.077 27	4.4	0.121	63.5	0.132	78.3	0.117	58.1
$^{23}Na^{19}F$	0.064 36	0.063 22	1.8	0.077	19.6	0.078	21.2	0.075	16.5
$^{23}Na^{35}Cl$	0.059 63	0.060 05	0.7	0.071	19.1	0.082	37.5	0.076	27.4
$^{23}Na^{79}Br$	0.053 1	0.053 14	0.0	0.073	37.7	0.076	43.4	0.071	34.0
$^{23}Na^{127}I$	0.050 7	0.050 44	0.5	0.074	45.9	0.078	53.8	0.074	45.9
$^{39}K^{19}F$	0.068 41	0.068 83	0.6	0.075	8.9	0.076	10.4	0.076	10.4
$^{39}K^{35}Cl$	0.059 66	0.059 69	0.0	0.072	20.7	0.074	24.0	0.072	20.7
$^{39}K^{79}Br$	0.050 25	0.049 72	1.0	0.067	33.3	0.065	29.3	0.063	25.4
$^{39}K^{127}I$		0.045 54		0.064		0.065		0.063	
$^{85}Rb^{19}F$	0.066 50	0.066 26	0.3	0.077	15.8	0.072	8.3	0.073	9.8
$^{85}Rb^{35}Cl$	0.054	0.054 15	0.0	0.068	25.9	0.066	22.2	0.065	20.4
$^{85}Rb^{79}Br$		0.041 49		0.056					
$^{85}Rb^{127}I$		0.035 60		0.053					
$^{133}Cs^{19}F$	0.072 29	0.072 75	0.6	0.078	7.9	0.074	2.4	0.075	3.7
$^{133}Cs^{35}Cl$	0.056	0.057 61	2.8	0.069	23.2	0.065	16.1	0.065	16.1
$^{133}Cs^{79}Br$		0.041 53		0.054					
$^{133}Cs^{127}I$		0.033 83		0.045		0.046		0.046	
		⟨% error⟩	1.5		26.7		30.4		24.0

[a] See Table 1 for experimental dipole moment references.

The principal differences among the various B-R models lie in the second term, that representing charge polarization. These differences are associated with the particular choices of polarizabilities. The Rittner model uses separated ion polarizabilities. These tend to subtract too much from the dipole moment. The more covalent the molecule, the further below the experimental μ_e is the value predicted by the Rittner model as can be seen by comparing columns 2 and 8 of Table VIII. DeWijn observed this behavior and deduced that it was due to the quenching of orbitals in the halogen ion directed along the internuclear axis. Thus he used halogen polarizabilities which were two-thirds the magnitude of the ionic polarizabilities. The resultant average error in μ_e computed with his model is quite small. Brumer and Karplus took a different approach. They postulated that nonbonding overlapping should affect the polarizability. So they introduced a polarizability which was exponentially dependent on R, and called the resultant model a dipole distortion model. The constant appearing in the exponential was chosen by demanding that the model give the correct μ_e.

Regarding the third major factor influencing the dipole moment, that due to nonbonding overlapping, none of the B-R models has a term which directly describes this. However, the dipole distortion model indirectly attempts to describe this phenomenon.

What are additional consequences of the shortcomings in the B-R models? First of all, predicted dipole moment slopes are too high since the polarizability term has to overcompensate for the leading term R. This fact is demonstrated in Table X where we have tabulated slopes computed with the derivatives of eq 12, the T-Rittner model, and eq 3 all evaluated at R_e. The average error in the T-Rittner model is 42.4% while eq 12 yields an average error of 1.6%. Notice that the slopes computed with the T-Rittner model are, in all cases, too large and that the error correlates with the effective charge transferred in the particular molecule.

To further illustrate this point, consider eq 4. By direct substitution it can be shown that the term α, representing the slope, contributes an order of magnitude more to μ_I than the term β representing the curvature. Thus μ_I computed with the B-R models must be considerably larger than those observed experimentally. That such is the case can be seen by examining

Table X. Comparison of Slopes of Dipole Moment Curves Evaluated at R_e

	$(d\mu/d\xi)\|\xi = 0$				
Molecule[a]	Exptl	T-Ritt	|% error|	Eq 58	|% error|
LiCl	8.4818	11.74	38.4	8.7118	2.7
NaF	8.0053	12.43	55.2	7.8726	1.7
NaCl	10.7967	18.01	67.6	10.9365	1.3
KF	11.1612	14.27	27.8	11.2462	0.7
KCl	13.2106	18.92	43.2	13.5080	2.1
RbF	12.3755	15.50	22.0	12.5426	1.3
		⟨% error⟩	42.4		1.6

columns 2, 5, 7, and 9 of Table IX. In all cases the B-R models predict values which are greater than the experimental values and in all cases the error is roughly proportional to the amount by which f varies from unity for a given molecule.

Not unexpectedly, the curvatures predicted by B-R models are quite far from those determined experimentally. To illustrate, the average experimental curvature for the molecules listed in Table X is about 1.1 debye bohrs^{-2} while eq 12 yields an average of 1.09. The T-Rittner and dipole distortion models yield values more than ten times this amount.

General Reliability of Constants

An examination of the full dipole moment model suggests several alternative approximations. It is worthwhile to investigate some of these in order to obtain a feeling for the general reliability and reproducibility of the results based on eq 12. The available experimental data, however, place restrictions on the number and types of terms which can be included in a model.

The models we investigated had the general form

$$\mu = fR\left(1 - \frac{a}{R^3}\right) + \frac{c}{R^n} + ke^{\alpha R} \qquad (27)$$

All constants were determined analytically by equating various orders of derivatives of eq 27 and 3 evaluated at R_e. We ascertained the following. (1) The values of f were fairly insen-

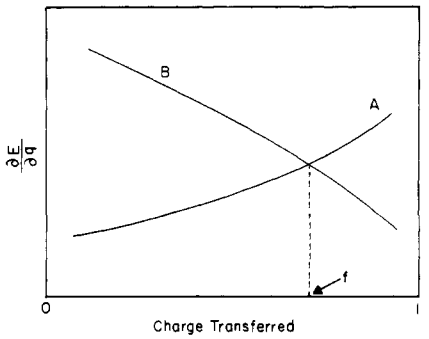

Figure 5. Schematic of differential changes in ionization potential and electron affinity vs. charge transferred. Curve A represents $\partial E_X/\partial q$ while curve B represents $-\partial E_M/\partial q$. The projection of the intersection onto the abscissa corresponds to the polarity of the molecule AB.

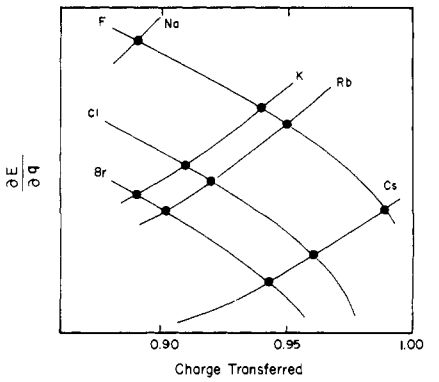

Figure 6. Variation of $\partial E/\partial q$ with charge transferred for alkali and halogen atoms.

sitive to the particular model. All models gave f's which were differences of atomic parameters. The magnitudes of the f's in all cases ranged from approximately 0.75 to 1.0 in a manner predictable from the periodic table. (2) The a coefficient approximated a sum of atomic polarizability in all cases. The model $fR(1 - a/R^3) + c/R^4$ yielded polarizabilities which did not require a coupling constant k_f. The cube roots of these polarizabilities correlated with Pauling's ionic radii with a correlation coefficient of 0.9995. (3) Inclusion of the term $ke^{\alpha R}$ led to inconclusive results. The four-term model yielded a fourth-order equation in α. the solutions to this equation were highly sensitive to extremely small variations in the experimental data. Consequently we had little confidence in the resultant constants. In general, the f's obtained when $ke^{\alpha R}$ was included were slightly higher than when it was excluded.

In principle the constants can be determined from ab initio calculations. We have determined f's for a few alkali halide molecules using SCF-LCAO-MO results.[21] These yield f's slightly higher than those given in Table III. This is expected since single-determinant SCF wave functions dissociate to an ionic state.

Bond Polarity and Bond Covalency

Frequent attempts to formulate criteria for resolving chemical bonds into ionic and covalent categories have been thwarted by the fact that molecular charge distributions are governed by a multitude of interactions. Success requires a proper deconvolution of these factors and a clear understanding of their relative contributions to charge rearrangements.

In the full dipole moment model two quantities f and c appear. As was pointed out, f is a direct measure of the charge transferred during bond formation and c is a measure of the number of shared electron pairs. As such it is reasonable to refer to f as the bond polarity or ionic bond number and to c as the bond covalency or covalent bond number. In singly bonded molecules f ranges in magnitude from unity for ion pairs to zero for homonuclear diatomic molecules while c ranges from zero for ion pairs to one in hypothetical singly bonded diatomic molecules in which two electrons are associated with the central region. We suggest that f and c are ideally suited to be the measure of the degree to which a bond be considered ionic or covalent. As was shown in paper 1, f is simply related to partial charges by the equation $f = (q_A - q_B)/2$ while $c = (q_A + q_B)/2$. Clearly c is orthogonal to f, a prerequisite if the classification of bonds into ionic and covalent categories is to have meaning in a quantitative sense.

In terms of c and f, the partial charges in a diatomic molecule are given by $q_A = c + f$ and $q_B = c - f$. These equations represent a simple, relatively nonarbitrary, method of determining partial ionic charges from experimental data. The polarity is determined from dipole moment data. Values of the covalency should be extractible from potential curve or quadrupole coupling constant measurements. Details of this procedure will be investigated in future papers.

A. Differential Charge Affinity. An interesting fact emerges from an examination of the bond polarities of the alkali halides. Not only are the f's related to partial charges they are also computable using a set of atomic q_α's. To demonstrate we have tabulated q_α's (ideal charges) for alkali and halogen atoms in Table IV and used these to compute the polarities listed in column 2 of Table VI. Empirically determined f's are given in column 2 of Table III. The agreement between the computed and empirical values is quite good. The average disagreement is less than 1%.

What does this imply? Consider the following thought experiment. Suppose from an isolated atom A, a differential element of electron density δq is removed from the surrounding charge cloud resulting in a partially charged ion with a charge cloud similar to that acquired in a molecular environment. The energy of the atom will be increased by an amount $\partial E_A/\partial q\, dq$. Let us call the negative of this quantity the differential charge affinity. For a given differential charge, the change in energy will depend on the position of the atom in the periodic table. As charge builds up on the other side, the net gain in energy gradually decreases until at some point there is no advantage to shipping charge from one atom to the other. At this point the polarity of the molecule is determined.

In terms of differential charge affinity curves, this situation corresponds to the point at which the curve of one atom intersects the mirror image curve $\partial E_B(-q)/\partial q$ of the other. This is illustrated in Figure 5 where we plot $\partial E_A(q)/\partial q$ and $-\partial E_B(-q)/\partial q$ vs. charge (curves A and B, respectvely). The area under A represents the ionization potential while the area under B represents the electron affinity. The point of intersection projected onto the axis corresponds to the bond polarity or effective charge transferred f.

Viewing this from another perspective we can say that charge is transferred until the quantity

$$I(y) = \int_0^y \left(\frac{\partial E_A}{\partial q}(q) + \frac{\partial E_B}{\partial q}(-q)\right) dq \qquad (28)$$

reaches a minimum with respect to variation in y. At the minimum $y = f$. In Figure 6 we have plotted a schematic of $\partial E_M/\partial q$ and $\partial E_X(-q)/\partial q$ for several of the alkali and halogen atoms. The points of intersections projected onto the abscissa correspond to the measured f's. The additivity of the f's is explained by the approximate parallelism of the differential charge affinity curves. To test this hypothesis we have plotted q_M vs. ionization potential in Figure 7. Even though the ionization potential represents the total area under the curve, a linear relationship is evident suggesting that the lines in Figure 6 are parallel over most of the range of f. It should be stated

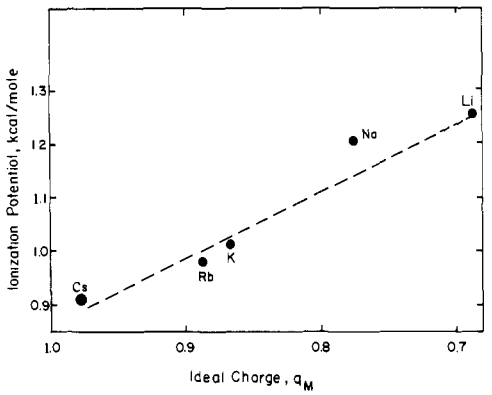

Figure 7. Variation of alkali atom ideal charge with ionization potential.

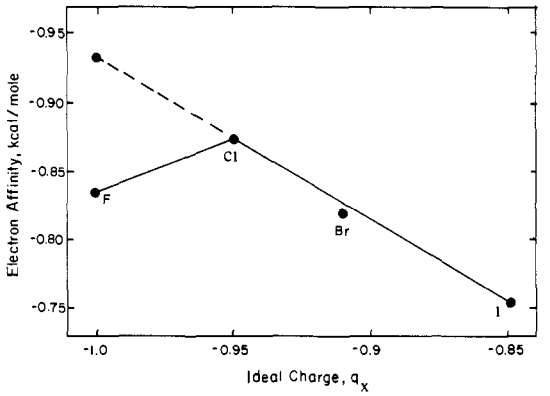

Figure 8. Variation of halide atom ideal charge with electron affinity.

that the schematic in Figure 6 assumes partial charges of $\pm f$. In reality the charges are $c + f$ and $c - f$. It is the energy expended in shipping $-dq$ from an ion with charge $c + f$ to one of charge $c - f$ that in this approximation determines the end of charge transfer. In Figure 8 we have plotted the electron affinity of the halide atoms vs. q_X, the ideal charge. This plot is linear except for fluorine. The implication of this is that the differential charge affinity curve of fluorine drops below that of chlorine when the electron charge approaches one. Substituting linear relationships between the q's and the ionization potential and electron affinity into $f = (q_A - q_B)/2$ leads to the relationship

$$f = 0.974\,48 - 0.004\,35(IP_M - EA_X) \qquad (29)$$

where IP_M represents the ionization potential of the metal and EA_X represents the halogen electron affinity except for fluorine[17] where it equals the electron affinity plus 9.486 kcal mol^{-1}. This equation yields f's with an average error of about 1.5%.

The result $f \approx 1 - C(IP_M - EA_X)$ is reasonable. If, in a singly bonded diatomic molecule, one atom has an ionization potential equal to the electron affinity of the other, the electron would be expected to transfer completely, with $f = 1$. In general, the amount of charge transferred should be related to the difference between the ionization potential and electron affinity. Since the electron affinity of fluorine is less than that of chlorine this leads to the anomalous prediction that fluorides would be less ionic than the corresponding chlorides, although this is not the case. That this anomaly does not materialize can be attributed to the role played by covalent charge transfer in determining the partial charge on the negative ion. The actual effective charge $c - f$ on fluorine is considerably less than -1 in the alkali halides.

B. Relationship of Commonly Used Electronegativity Scales to Differential Charge Affinity Curves. The chemist calls the relative ability of atoms in a molecule to attract electrons the electronegativity. Since differential charge affinity curves give a direct measure of this ability they should be closely related to electronegativity scales. Let us examine this relationship.

Several scales of electronegativity have been constructed. The two most widely used are those of Pauling[23] and Mulliken.[24] Pauling's scale is based on the assumption that the difference between the energy $D(A\text{-}B)$ of the bond between two atoms A and B and the energy expected for a normal covalent bond $\frac{1}{2}\{D(A\text{-}A) + D(B\text{-}B)\}$ increases as the difference in their electronegativities increases. In algebraic form

$$23(X_A - X_B)^2 = D(A\text{-}B) - \tfrac{1}{2}[D(A\text{-}A) + D(B\text{-}B)] \qquad (30)$$

where X_α is the electronegativity of atom α.

Mulliken bases his scale on the fact that the average ionization potential IP and electron affinity EA of an atom should be a measure of the electron attraction of the neutral atom and hence its electronegativity, or $X_\alpha = (IP_\alpha + EA_\alpha)/2$. Scales based on these somewhat different formulas are surprisingly similar. This can be seen by an examination of Table XI where we have tabulated ionization potentials, electron affinities, the average of the two quantities, and Pauling's value of the electronegativity for a series of atoms.

Table XI. Comparison of Electronegativity with the Average of Ionization Energy and Electron Affinity[a]

Atom	Ionization potential	Electron affinity	Sum/125	X^P
F	403.3	83.5	3.90	4.0
Cl	300.3	87.3	3.10	3.0
Br	274.6	82.0	2.86	7.8
I	242.2	75.7	2.54	2.5
H	315.0	17.8	2.66	2.1
Li	125.8	0	1.01	1.0
Na	120.0	0	0.96	0.9
K	101.6	0	0.81	0.8
Rb	97.8	0	0.78	0.8
Cs	91.3	0	0.73	0.7

[a] L. Pauling, "The Nature of the Chemical Bond", 3rd ed, Cornell University Press, Ithaca, N.Y., 1960, p 96.

A relationship between differential charge affinity curves and electronegativity scales is most easily obtained by utilizing Mulliken's scale. Substituting for IP_α and EA_α we obtain

$$X_\alpha = \tfrac{1}{2}\int_0^1 \left[\frac{\partial E_\alpha}{\partial q}(q) - \frac{\partial E_\alpha}{\partial q}(-q)\right] dq \qquad (31)$$

This relationship implies that the Mulliken scale of electronegativities is an integrated averaging of the detailed information pertaining to bond polarity extractable from differential charge affinity curves.

C. Bond Polarity and Ionic Character. According to Pauling the ionic character of a molecule is roughly approximated by the equation

$$\delta_p = \mu_e/R_e \qquad (32)$$

Let us examine the relationship between this quantity and the polarity f. Taking the zeroth, first, and second derivatives of eq 12 and solving for f we obtain

$$f = \tfrac{5}{9}\frac{\mu_e}{R_e} + \tfrac{4}{9}\mu_e' + \tfrac{1}{18}\mu_e'' R_e \qquad (33)$$

This equation suggests that several factors effect the bond polarity. The term μ_e/R_e reflects the relative magnitude of the dipole moment at R_e compared to the point charge dipole eR_e.

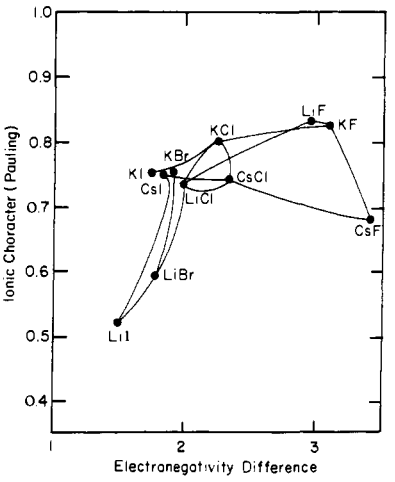

Figure 9. Relationship between Pauling ionic character and electronegativity differences.

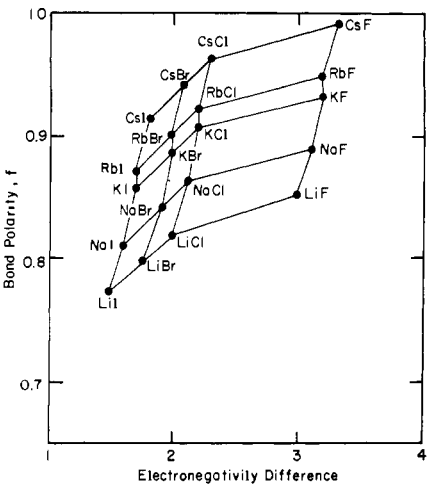

Figure 10. Relationship between bond polarity and electronegativity difference.

The term μ_e' represents the slope of the ipole moment curve at R_e and μ_e'' the curvature. The Pauling approximation only takes the first of these into account.

It is not unreasonable to expect some correlation between bond polarity, ionic character, and electronegativity differences since all of these are related to the tendency of a bond to polarize. In Figure 9 we have plotted Pauling's approximation vs. electronegativity differences. We have connected molecules containing similar alkali or halogen atoms. Although there are certain trends, the figure is generally scrambled. In Figure 10 the bond polarity is plotted against electronegativity differences. The pattern is quite symmetric confirming the close relationship between the two quantities.

To account for the unreasonable trends displayed by Figure 9 we can solve eq 12 for f in terms of δ_p

$$f \approx \delta_p \left(1 - \frac{\alpha_A + \alpha_B}{R^3}\right)^{-1} \tag{34}$$

It is evident from this equation that the low apparent ionic character of CsF for example is due to the neglect of a rather large Cs polarizability.

Discussion

The semiempirical dipole moment model examined in this paper appears to represent experimental data more accurately than the models of Rittner, DeWijn, Brumer, and Karplus. Its major advantage is its representation of transfer of a partial charge during bond formation, the amount varying in a systematic way with the periodic table.

The analysis in this paper partially confirms the correctness of the model developed quantum mechanically in the first paper of this series, in which partial charge transfer is also represented. More accurate and extensive data are required to test other features of the quantum mechanical model.

It is useful to have available approximate formulas which can be used to ascertain the relative contributions from charge transfer, charge polarization, and charge overlap effects from experimental dipole moment curves. This can be obtained by equating the zeroth, first, and second derivatives of eq 3 and 12 evaluated at R_e and solving for the appropriate coefficient. We find, in addition to eq 33,

$$f(\alpha_A + \alpha_B)/R_e^2 = \tfrac{5}{9}\frac{\mu_e}{R_e} - \tfrac{5}{9}\mu_e' - \tfrac{1}{9}\mu_e''R_e \tag{35}$$

and

$$f\exp(\gamma_A + \gamma_B)/R_e^5 = -\tfrac{1}{9}\frac{\mu_e}{R_e} + \tfrac{1}{9}\mu_e' + \tfrac{1}{18}\mu_e''R_e \tag{36}$$

Equation 33 represents, effectively, a simple relationship between bond polarity and experimentally measurable dipole moment data. These equations should prove useful in clearing up several paradoxes reported in the literature.[25] For example, O'Hare and Wahl suggest that their calculated value of the dipole moment of carbon monofluoride

$$\mu = 0.471 - 3.561(R - R_e) - 0.249(R - R_e)^2 + 0.169(R - R_e)^3 \tag{37}$$

implies that the charge distribution corresponds to C^-F^+. Such a suggestion, based on an oversimplified picture of the relationships of dipole moments to charge distributions, runs contrary to their chemical intuition and to ours.

An interpretation more in accord with chemical experience can be obtained by an application of the above equations. According to eq 33 the effective charge transferred in CF is 0.605 with polarity C^+F^-. Contributions to μ_e from the charge transfer, charge polarization, and charge overlap terms are −3.65, 5.28, and −1.15 D, respectively. The dipole moment associated with the partial charges on each atom is thus quite large. The polarization term is clearly a prime contributor to the anomalous dipole moment near R_e. It should be stated, however, that the application of the full model would probably be more appropriate to this problem due to the large covalent effects present in CF.

Several points brought out in this paper are speculative and require confirmatory research and additional development. Nevertheless, we are reasonably confident of the correctness of our basic hypothesis. Part of this confidence is based on the fact that analysis of molecular wave functions yield results in fair agreement with ours.

For example, Bader, Henneker, and Cade[26] suggest that it is possible to obtain a fair approximation to the polarity of a bond by examining density distributions to determine the buildup of charge in various regions. Following this procedure they determine a polarity of 0.85 for LiF using SCF wave functions. This is close to our value of 0.84.

An analysis of NaF based on density difference maps[27] suggests that fluorine has a partial charge of 0.6 ± 10% and this charge is constant between R = 6.0 and 3.1. This partial charge is in accord with a charge which would be predicted using the methods outlined in this paper.

An examination of density difference profiles of alkali halide molecules[27] using SCF wave functions[21] indicates that the cross section in the area of the Li nucleus is very nearly the same whether in LiF, LiCl, or LiBr and the Cl cross section is remarkably similar in LiCl, NaCl, and KCl.

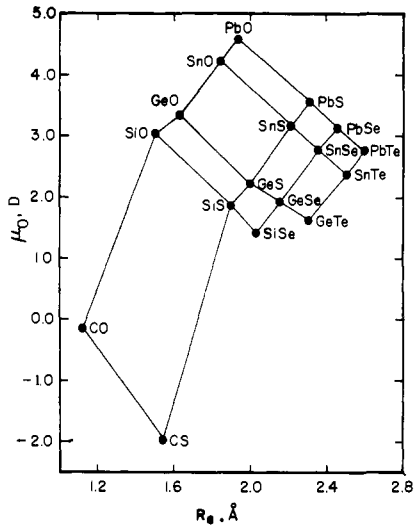

Figure 11. Variation of μ_0 with R_e for Group 4 monocholcogenides.

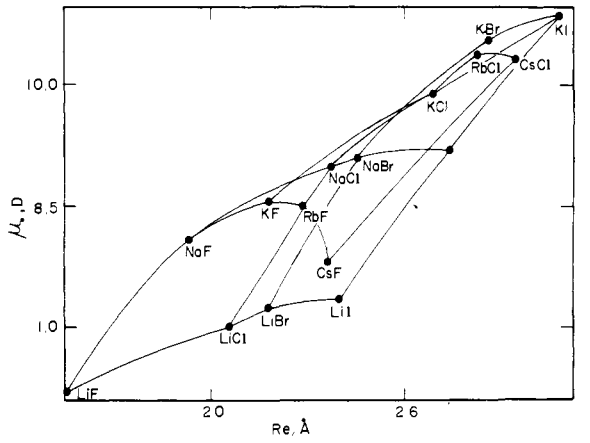

Figure 12. Variation of μ_0 with R_e for alkali halides.

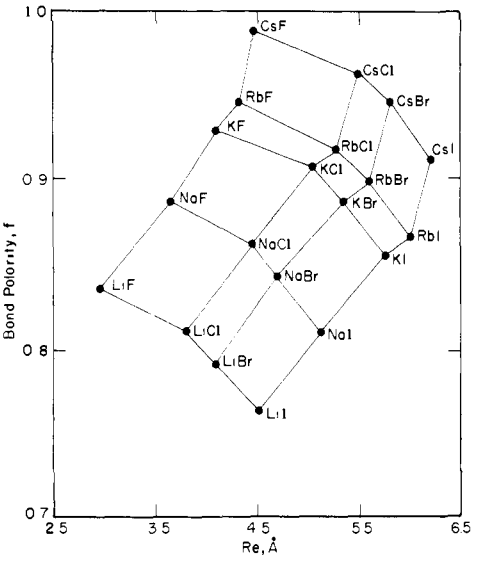

Figure 13. Variation of polarity with R_e for alkali halides.

Bader and Srebrenik[28] partition a molecule in such a way that the virial relationship between the average kinetic and potential energies observed for a total molecular system is found to hold for individual fragments. These fragments are defined in terms of an observable property of the charge distribution. One result of such a partitioning is the constancy of certain physical properties such as the fragmented charge distributions.

Experimental confirmation is also available. For example, μ_0/R_e approximately equals 0.27, 0.034, and 0.22 for CsNa, NaLi, and KLi, respectively.[29] If we arbitrarily assign $q_{Cs} = 1$ and assume the polarizability and charge overlap effect on the dipole moment are negligible, we obtain $q_{Li} = 0.372$, $q_{Na} = 0.46$, and $q_K = 0.832$. Using q_{Na} and q_K to calculate f we obtain an approximate bond plarity of 0.176 for KNa. The observed value is 0.17. Similarly we predict a bond polarity of 0.31 for CsLi. Using $R_e = 3.62$ by Badger's Rule we obtain an estimated dipole moment $\mu = 5.28$ D for CsLi. The dipole moment has not yet been measured for this molecule.

Hoeft, Lovas, Tiemann, and Toerring[30] have determined that a plot of μ_0 and R_e for the group 4 monochalcogenides yields a series of straight lines (see Figure 11). They suggest that a common fundamental property should explain the variation of electron distribution in the series of compounds of C, Si, Ge, Sn, and Pb. According to our views this property is the differential charge affinity. For comparison they plot μ_0 and R_e for the strongly polar alkali halides (see Figure 12), obtaining a series of curves. They interpret this nonlinear structure as evidence for a fundamental difference in bonding between the I/VII and IV/VI molecules. We suggest a different interpretation. As measurements of dipole moment curves accumulate, a systematic trend in polarities across the periodic table should emerge. Figure 12 can be viewed as a transparent sheet whose upper left corner (CsF) is bent toward the observer. To understand why the sheet is warped it is instructive to consider Figure 13 where we plot f and R_e. The figure is similar to Figure 11. A plot of fR_e vs. R_e also yields a regular grid. It is easily shown that

$$\mu_0 \approx fR_e - \frac{q_A\alpha_B - q_B\alpha_A}{R_e^2} \qquad (38)$$

Thus to the extent μ_0 approximates the behavior of fR_e, the grid is expected to be linear. A warped grid is due to systematic variations in the importance of the second and higher order terms.

We are currently involved in an analysis of potential energy curves and electric field gradients of diatomic molecules. This research should provide additional information regarding the polarity and covalency and their roles in chemical bonding.

Acknowledgment. The authors wish to thank Dr. Mac Milleur and Mr. Jerry Anderson for computational aid, Dr. Luis Kahn and Mr. Rudolf Goldflam for helpful comments, and Dr. C. W. Kern for a careful reading and criticism of the original manuscript. In addition, they wish to acknowledge the support of Battelle Memorial Institute and the Robert A. Welch Foundation through Grant No. E-397.

References and Notes

(1) (a) Address correspondence to the University of Houston; (b) Battelle Memorial Institute; (c) University of Houston.
(2) R. L. Matcha and S. King, *J. Am. Chem. Soc.*, preceding paper in this issue.
(3) (a) E. S. Rittner, *J. Chem. Phys.*, **19**, 1030 (1958); (b) R. M. Herman and S. Short, *ibid.*, **48**, 1266 (1968).
(4) G. Graff, R. Schonwasser, and M. Tonutiti, *Z. Phys.* **199**, 157 (1967).
(5) L. Wharton, W. Klemperer, L. P. Gold, R. Strauch, J. J. Gallagher, and V. E. Derr, *J. Chem. Phys.*, **38**, 1203 (1963).
(6) C. D. Hollowell, A. J. Hebert, and K. Street, Jr., *J. Chem. Phys.*, **41**, 3540 (1964).
(7) D. R. Lide, P. Cahill, and L. P. Gold, *J. Chem. Phys.*, **40**, 156 (1964).
(8) W. Klemperer, W. G. Norris, and A. Buchler, *J. Chem. Phys.*, **33**, 1534 (1960).
(9) P. L. Clouser and W. Gordy, *Phys. Rev.*, **134**, A863 (1964).
(10) J. R. Rusk and W. Gordy, *Phys. Rev.*, **127**, 817 (1962).
(11) R. van Wachem, F. H. de Leeuw, and A. Dymanus, *J. Chem. Phys.*, **47**, 2256 (1967).
(12) A. J. Hebert, F. J. Lovas, C. A. Melendres, C. D. Hollowell, T. L. Story, and K. Street, *J. Chem. Phys.*, **48**, 2824 (1968).

(13) S. E. Veazey and W. Gordy, *Phys. Rev.*, **138**, A1303 (1965).
(14) A. Honig, M. Mandel, M. L. Stitch, and C. H. Townes, *Phys. Rev.*, **96**, 629 (1954).
(15) A. J. Hebert, F. W. Breivogel, and K. Street, *J. Chem. Phys.*, **41**, 2368 (1964).
(16) F. W. Breivogel, A. J. Hebert, and K. Street, *J. Chem. Phys.*, **42**, 1555 (1965).
(17) Fluorides are notorious for anomalous behavior [see for example P. Politzer, *J. Am. Chem. Soc.*, **91**, 6235 (1969); R. S. Evans and J. E. Huhley, *Chem. Phys. Lett.*, **19**, 114 (1973)]. However the dichotomous (LiF–LiCl) f values are probably not related to abnormalities associated with fluorine. More likely, they result from a combination of factors including differential ionic radii and covalent change buildup. An examination of eq. 1 reveals that the term proportional to R in the quantum mechanically derived dipole moment model is $f + 2cz_{cv}/R$. In most of the alkali halides the covalent factor is negligible due to a combination of either a small c or small z_{cv}. However in the lithium halides both c and z_{cv} are nonnegligible. Thus in Figure 2, the appearance of the LiCl f in a position lower than would be predicted by the intersection of a vertical line and a slanted line through LiF is a result of an increasingly important covalent contribution going down a column in the lithium halides.
(18) A. von Hippel, "Dielectrics and Waves", Wiley, New York, N.Y., 1954.
(19) P. Brumer and M. Karplus, *J. Chem. Phys.*, **58**, 3903 (1973).
(20) H. E. DeWijn, *J. Chem. Phys.*, **44**, 810 (1966).
(21) R. L. Matcha, *J. Chem. Phys.*, **47**, 4595, 5295 (1967); **48**, 335 (1968); **49**, 1264 (1968); **53**, 485, 4490 (1970).
(22) R. L. Matcha and R. K. Nesbet, *Phys. Rev.*, **160**, 72 (1967).
(23) L. Pauling, "The Nature of the Chemical Bond", 3rd ed, Cornell University Press, Ithaca, N.Y., 1960, p 78.
(24) R. S. Mulliken, *J. Chem. Phys.*, **2**, 782 (1934).
(25) P. O. Hare and A. C. Wahl, *J. Chem. Phys.*, **55**, 666 (1971).
(26) R. F. W. Bader, W. H. Henneker, and P. E. Cade, *J. Chem. Phys.*, **46**, 3341 (1967).
(27) L. A. Curtiss, C. W. Kern, and R. L. Matcha, *J. Chem. Phys.*, **63**, 1621 (1975).
(28) S. Srebrenik and R. F. W. Bader, *J. Chem. Phys.*, **61**, 2536 (1974).
(29) P. Dagidigion and L. Wharton, *J. Chem. Phys.*, **57**, 1487 (1972).
(30) J. Hoeft, F. J. Lovas, E. Tiemann, and T. Toerring, *J. Chem. Phys.*, **53**, 2736 (1970).

A Localized Molecular Orbital Interpretation of the Dipole Moment Derivatives of Ammonia. A Reexamination of the Bond Moment Model Description of Infrared Intensities

Roy E. Bruns,* A. B. M. S. Bassi, and Paul M. Kuznesof

Contribution from the Instituto de Quimica, Universidade Estadual de Campinas, 13.100 Campinas, SP, Brazil. *Received August 19, 1975*

Abstract: Preferred experimental values for the dipole moment derivatives of ammonia have been selected on the basis of the CNDO calculated signs for these quantities. Bond dipole moment values and directions have been calculated from the localized molecular orbital representations of the CNDO canonical MO's. The relative merits of the bond moment model assumptions pertinent to the interpretation of infrared intensities are assessed in terms of the theoretical results. The lone pair moment contributions to the dipole moment derivatives are also examined.

The comparison and interpretation of infrared gas phase intensity data have frequently been affected through use of the bond moment model. Bond moments evaluated with the aid of these data are not necessarily expected to agree with those bond moments whose vector sums are equal to the equilibrium dipole moments. Rather, a most important role of this model is to emphasize the differences between the equilibrium and the various infrared bond moments. These latter moments not only have different values for the same type of bond in different molecules, but also upon their evaluation from infrared intensities corresponding to normal coordinates of different symmetry for the same molecule.

Because a number of factors can produce different bond moment values, the reasons for the limited success of the bond moment model are not well understood. In its most restrictive form the model implies:[1,2] (1) when a bond is stretched by dr, a moment $(\partial\mu/\partial r)\,dr$ is produced in the direction of the bond, (2) when a bond is bent through an angle $d\theta$, a moment $\mu_0\,d\theta$ is produced in the plane of bending perpendicular to the direction of the bond, and (3) when one bond is stretched or bent no changes occur in the other bonds. Differences in the bond moment values obviously can result from inaccuracies in any one of these assumptions. More realistically all three assumptions are not rigorously valid.

A quantum mechanical assessment of the relative merits of the above assumptions is clearly desirable. The approach we have taken is one in which the molecular orbitals (MO's) may be localized on the various bonds and isolated electron pairs in the molecule. Since standard SCF–MO methods yield orbitals which are delocalized over the entire molecule in a manner consistent with molecular symmetry, spatial transformations of these canonical MO's (CMO's) to localized MO's (LMO's) must be performed; a variety of techniques have been devised.[3] The LMO's can be used to calculate dipole moments for the individual bonds of the molecule at its equilibrium and vibrationally distorted geometries. Although the relative accuracies of the assumptions involved in the bond moment models are expected to vary for different molecules, the results for any one molecule should contribute to our understanding of why these models are too simple to allow an accurate general interpretation of infrared intensities.

We have chosen to study the infrared intensity data of ammonia[4] for the following reasons. First, the intensities can be interpreted in terms of the changes in the dipole moments of the NH bonds and the changes in the electronic distribution of the lone pair on nitrogen. Second, since CNDO[5] determination of the signs of the dipole moment derivatives with respect to the normal coordinates, the $\partial\mu/\partial Q_i$, have been reported for only the A_1 symmetry species,[6] it is useful to obtain CNDO estimates of the derivatives for the E species.

Calculations

The CNDO calculated dipole moment derivatives with respect to the symmetry coordinates, the $\partial\mu/\partial S_j$, were obtained in the usual manner.[6,7] Maximum displacements of 0.02 Å and 2° from the equilibrium geometry were used to determine the symmetry coordinate distortions. The symmetry coordinates were taken to be functions of the internal coordinates equal to